Biochimica et Biophysica Acta, 1024 (1990) 159–166
Elsevier

BBAMEM 74824

Lanthanide(III)-phosphatidic acid complexes: binding site heterogeneity and phase separation

Joanne Sun and Matthew Petersheim

Chemistry Department, Seton Hall University, South Orange, NJ (U.S.A.)

(Received 21 November 1989)

Key words: Phosphatidic acid; Cation binding; Phase separation; Lanthanide; Luminescence; Resonance energy transfer

The luminescent lanthanides are potentially useful probes of cation-induced events involving phospholipid membranes. In this work, the spectroscopic properties of Tb^{3+}, Ce^{3+} and Eu^{3+} are shown to be complementary in defining three forms of complex with phosphatidic acid vesicles. Ce^{3+}, in particular, is useful for studying dilute cation-lipid complexes because it has strong excitation bands in the near ultraviolet. In addition to providing a means for detecting chemically distinct forms of lanthanide-lipid complexes, the luminescence can be used to monitor cation-induced lateral segregation. Ce^{3+} to Tb^{3+} energy transfer was observed at lanthanide levels as low as 1:1000 Ln^{3+}/phosphatidic acid, indicating clustering or phase separation. Initial clustering occurs on a subsecond timescale, followed by a much slower aggregation continuing for several minutes to hours. Addition of a chelator results in slow release of the lanthanides. In the case of the dioleoylphosphatidic acid complexes, release is bimodal and indicative of cation entrapment; dimyristoylphosphatidic acid complexes exhibit this behavior only at high temperatures. These observations are consistent with the relative tendencies of these two lipids to form the H_{II} phase. This work sets the foundation for experiments designed to determine the size of nucleation sites for cation-induced events such as intramembrane inverted micelle formation and membrane fusion.

Introduction

The coordination chemistry of polyvalent cations bound to membrane phospholipids may be important in determining the lateral chemical potential of the lipid [1–6], conversion to nonlamellar states [7–12], and definition of contacts between adjacent membrane surfaces [13–15]. Direct observation of dilute or transient forms of these phospholipid complexes with cations such as Ca^{2+} is difficult because the cation has no convenient spectroscopic properties. Physical properties of the lipid that would be useful in defining the complexes are generally dominated by the free lipid unless the complex represents several mole-percent. For this reason the luminescent lanthanides have been investigated as probes of cation-lipid interactions [16–21]. The trivalent lanthanides are hard Lewis acids and have ionic radii close to that of Ca^{2+}. Although the lanthanides are unlikely to be important in the biochemical processes normally ascribed to Ca^{2+}, they have been shown to substitute into the same sites on Ca^{2+}-binding proteins [22–26] and are efficient at inducing membrane fusion [5,6,15,27].

Saris [16] found the luminescence intensity of Eu^{3+} to vary with the identity of the phospholipid headgroup and observed energy transfer between Tb^{3+} and Eu^{3+} in a mixed lipid system. Herrmann et al. [17] used a dye-laser system to obtain high resolution excitation spectra and luminescence lifetimes for Eu^{3+} complexes with several pure phospholipids. Their results indicate that there is generally one dominant form of complex at stoichiometric levels of bound lanthanide and that 1–2 water molecules remain in the coordination sphere. The aquo-Eu^{3+} species has roughly 9 coordinating water molecules [25]. Studies exploiting the sensitivity of the Tb^{3+} 4f to 5d excitation bands to changes in ligand field demonstrate that there is more than one type of lanthanide complex formed with each phospholipid species. The populations of the complexes depend on either the level of bound lanthanide or the degree of protonation of the lipid [18–21].

In one of the Tb^{3+} studies [19] it was observed that near pH 7 the lanthanide forms at least two different

Abbreviations: DMPA, dimyristoylphosphatidic acid; DOPA, dioleoylphosphatidic acid; DPPA, dipalmitoylphosphatidic acid; POPA, *sn*-1-palmitoyl-2-oleoylphosphatidic acid; Ln^{3+}, trivalent lanthanide; EDTA, ethylenediaminetetraacetate.

Correspondence: M. Petersheim, Department of Chemistry, Seton Hall University, South Orange, NJ 07079, U.S.A.

complexes with dimyristoylphosphatidic acid (DMPA) while the evidence suggested dioleoylphosphatidic acid (DOPA) forms only a single type of complex. These two lipids differ in the pH dependence of the lamellar interfacial area per phosphate [28] and tendency to convert to nonlamellar structures in the presence of polyvalent cations [7–12]. The experiments presented here were intended to test whether the variation in Tb^{3+} coordination could be understood in terms of these established differences in the physical properties of the lipids. Lanthanide-lanthanide energy transfer experiments were explored as a means for detecting differences in the phase behavior of the lanthanide-lipid complexes for the two phosphatidic acid species.

Ce^{3+} is introduced as a sensitive probe of the cation binding site and very efficient energy transfer donor to Tb^{3+}. Because Ce^{3+} has allowed 4f to 5d absorption bands with extinction coefficients on the order of 1000 $M^{-1} \cdot cm^{-1}$ at wavelengths longer than 240 nm, emission studies with conventional fluorescence equipment yield intensities at least two orders of magnitude greater than that from the more common lanthanide probes, Tb^{3+} and Eu^{3+}. The allowed Tb^{3+} 4f to 5d bands generally occur at the edge of the Xe lamp emission profile and are more difficult to study. The Tb^{3+}-phosphatidic acid 4f to 5d excitation bands lying above 240 nm are apparently spin forbidden, with extinction coefficients on the order of 1 $M^{-1} \cdot cm^{-1}$ [19]. The 5d excited states in these Ce^{3+} and Tb^{3+} transitions are directly exposed to the ligand field and, as a consequence, the excitation bands are very responsive to changes in the coordination environment. The greater emission efficiency of Ce^{3+} is an important advantage for those interested in using the lanthanides to probe membrane events. It greatly relieves the instrumental demands for the spectroscopy, allowing studies on conventional fluorescence equipment at micromolar levels. Although the Eu^{3+}-lipid studies of Herrmann et al. [17] were also performed at micromolar levels, they employed a scanning dye laser as an excitation source. Attempts to obtain equivalent Eu^{3+} excitation spectra with the high resolution fluorescence spectrometer used in this work were unsuccessful. A more complete comparison of Ce^{3+} spectroscopic properties with those of the two more common probes, Tb^{3+} and Eu^{3+}, is presented elsewhere [26].

Materials and Methods

The dimyristoylphosphatidic acid and *sn*-1-palmitoyl-2-oleoylphosphatidic acid were purchased from Avanti Polar Lipids, Inc. (Pelham, AL) and dioleoylphosphatidic acid was purchased from Sigma Chemical Co. (St. Louis, MO). Lipid concentrations of stock aqueous suspensions were calculated from the weight of lipid used and 0.1 M NaCl was present in all samples. Analytical grade $TbCl_3$ and $CeCl_3$ were used and aqueous Eu^{3+} was prepared by dissolving Eu_2O_3 in a stoichiometric amount of perchloric acid.

The lipid suspensions were prepared as sonicated vesicles using glass vials mounted in a jacketted bath adaptor for a 300W Fisher sonic dismembrator. Individual samples were sonicated at a temperature above the gel to liquid crystal transition until the suspension was clear, usually 20 to 60 min. For all experiments except the kinetics studies of $Ce^{3+} \rightarrow Tb^{3+}$ energy transfer, the lipid suspension was sonicated a second time after addition of the lanthanide solution. The pH was adjusted with either hydrochloric acid or sodium hydroxide, followed by sonication. A 3 mm diameter combination glass electrode was used to measure the pH. In the kinetics experiments, 0.02 ml of a 0.2 mM Ce^{3+} and 0.2 mM Tb^{3+} solution (0.1 M NaCl) was added to 1.0 ml of 0.25 mM lipid (0.1 M NaCl) and the mixture was gently inverted ten times before observation.

Excitation and emission spectra for Ce^{3+} and Eu^{3+} were collected with a Spex Fluorolog 2 (Spex industries, Inc., Edison, NJ). Tb^{3+} excitation spectra and kinetic studies of $Ce^{3+} \rightarrow Tb^{3+}$ energy transfer were performed on a home-built instrument described elsewhere [20]. In all experiments, a quartz fluorescence cell was used with a 4 mm excitation path. The temperature was controlled with a circulating refrigerated bath and a jacketted cell holder; a digital thermometer with 0.1 C° precision was used to measure the temperature at the cell.

Infrared spectra were acquired with a Cygnus 25B Fourier transform infrared spectrometer from Mattson Instruments, Inc. (Madison, WI) using a thermoregulated transmission cell. Phosphorous-31 nuclear magnetic resonance experiments were performed on a QE-300 multinuclear NMR spectrometer from the General Electric Company (Fremont, California) using a 10 mm broad-band probe.

Results

Binding site heterogeneity

Excitation spectra for Tb^{3+} complexes with both DMPA and DOPA at low, medium and high pH are presented in Fig. 1; the lipid precipitates at or below pH 2. The features that change most noticeably in these Tb^{3+} spectra are 4f to 5d bands [19,29]. In addition to the two Tb^{3+}-DMPA complexes reported previously [19], the 310 nm excitation band present at high pH is indicative of a third form of the complex (Fig. 1). Excitation bands characteristic of these three Tb^{3+}-DMPA complexes are listed in Table I. Changes in the Tb^{3+}-DOPA excitation spectrum are subtler in comparison, which is consistent with the earlier observations [19].

Ce^{3+} was introduced in these studies as a possible donor in resonance energy transfer to Tb^{3+}. Excitation

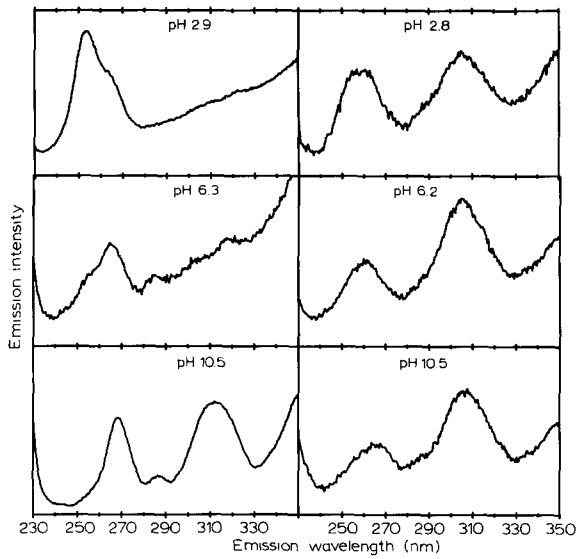

Fig. 1. pH-induced changes in Tb^{3+}-DMPA (left column) and Tb^{3+}-DOPA (right column) at 25 °C. All six are excitation spectra monitoring the 545 nm emission band of Tb^{3+}. The samples consisted of 2.0 mM lipid, 0.1 mM Tb^{3+} and 0.1 M NaCl and were sonicated after each pH adjustment.

TABLE I

Characteristic excitation bands for the three DMPA complexes

Ln^{3+}-DMPA complex	Excitation maxima [a]	
	Tb^{3+}	Ce^{3+}
low-pH	253 nm	293 nm [b]
	–	? [c]
mid-pH	264 nm	258 nm
	305 nm	298 nm
high-pH	270 nm	273 nm
	313 nm	309 nm

[a] Dominant excitation bands above 230 nm.

[b] The low-pH form for Ce^{3+}-DMPA was not well defined in the spectra. This band position was estimated by fitting the spectrum with four Gaussian functions using a nonlinear regression routine.

[c] The second band in the low-pH form of Ce^{3+}-DMPA was not fit well by the nonlinear regression, so no value is quoted here.

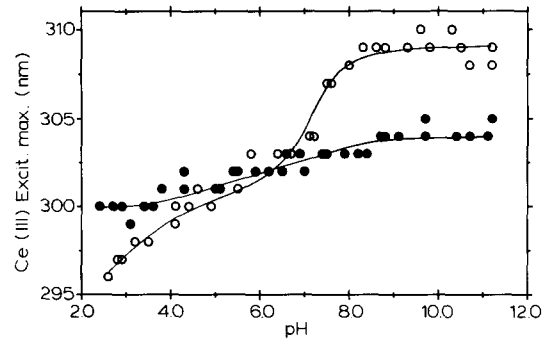

Fig. 3. Ce^{3+}-phosphatidic acid pH dependence. Position of the excitation maximum for Ce^{3+}-DMPA (empty circles) and Ce^{3+}-DOPA (filled circles) as a function of pH. The experimental conditions are those given in the caption for Fig. 2.

and emission spectra for this lanthanide consist solely of 4f to 5d transitions [26,30,31] and the emission intensity is generally two or more orders of magnitude greater than that for the other lanthanides. In the excitation spectrum for Ce^{3+}-phosphatidic acid species there are only two bands above 230 nm (Fig. 2). The dominant band in the Ce^{3+}-DMPA spectrum appears to shift continuously to longer wavelength with increasing pH, which is shown more clearly in Fig. 3. There is an inflection in the curve near pH 7 and another suggested by the data below pH 2.5. These observations indicate that Ce^{3+} also forms three different complexes with DMPA. Experiments with the mixed acylchain species, POPA, gave very nearly the same pH dependence for Ce^{3+}-POPA as for Ce^{3+}-DMPA. Table I contains estimates of band positions for all three forms of the complex. The plot of Ce^{3+}-DOPA band position in Fig. 3 reveals that there is a change in complexation with this lipid which is not as easily discerned in the Tb^{3+} spectra.

Eu^{3+} was included to ensure that the Tb^{3+} and Ce^{3+} studies could be compared with those of Saris [16] and

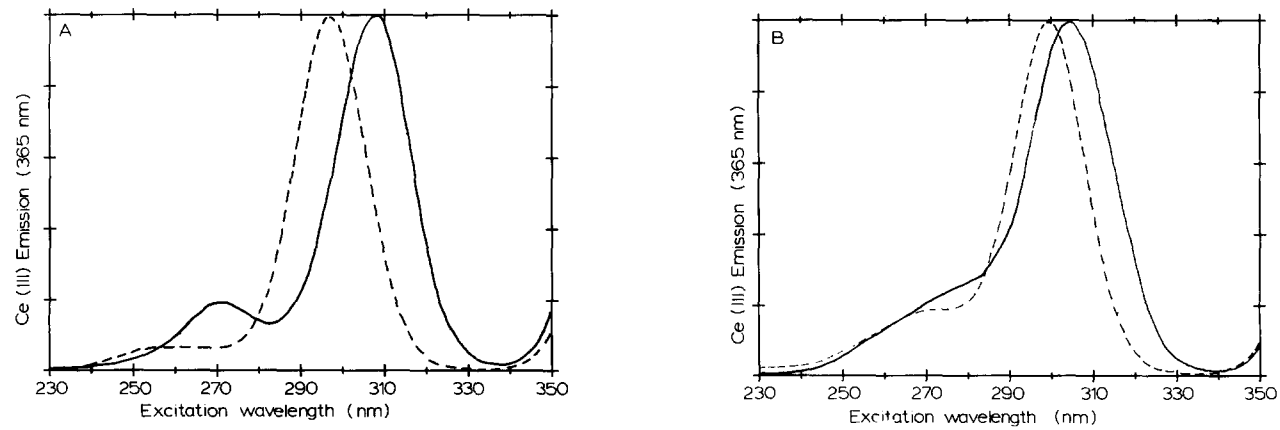

Fig. 2. pH-induced changes in (A) Ce^{3+}-DMPA and (B) Ce^{3+}-DOPA at 25 °C. The dashed line is the excitation spectrum for pH 2.8 and the solid line is for pH 11.2 in both figures; emission was monitored at 365 nm. The samples consisted of 0.25 mM lipid, 0.025 mM Ce^{3+} and 0.1 M NaCl and were sonicated after each pH adjustment.

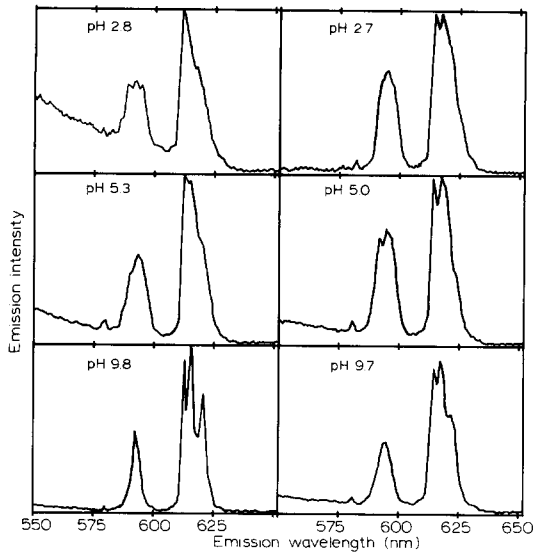

Fig. 4. pH-induced changes in Eu^{3+}-DMPA (left column) and Eu^{3+}-DOPA (right column) at 25°C. All six are emission spectra using excitation at 394 nm, the strongest Eu^{3+} absorption band. The samples consisted of 2.0 mM lipid, 0.1 mM Eu^{3+} and 0.1 M NaCl and were sonicated after each pH adjustment.

Hermann et al. [17]. Fig. 4 shows the emission spectra for Eu^{3+}-DMPA and Eu^{3+}-DOPA at low, mid, and high pH. The sharp bands of Eu^{3+}-DMPA near pH 10 suggest that there is a dominant form of the complex at high pH. The poorer band definition at lower pH is consistent with coexistence of two or more forms of the complex, as expected from the other lanthanide-DMPA studies. Likewise, Eu^{3+}-DOPA behaves much as expected with less dramatic changes in the spectral features than observed with the DMPA species.

The band shapes in the Eu^{3+}-DOPA and Tb^{3+}-DOPA spectra and the pH dependence of the Ce^{3+} excitation band indicate that a mixture of two DOPA complexes exist even near pH 11. This is strong evidence that these two species do not differ in the degree of protonation of the phosphates, or that the coordinating phosphates are completely aprotic over the entire pH range for DOPA. The two DOPA complexes appear to be very similar to the mid- and high-pH Ln^{3+}-DMPA species, based on the spectral features of all three lanthanides, suggesting that at least these two forms of the DMPA complexes are aprotic as well.

The formation of aprotic complexes in the pH range where most of the phosphates should be monoprotic is supported by repeated observations of a slow decrease in pH by nearly a full pH unit following addition of lanthanide. This has been observed with both DOPA and DMPA, where the lipid is 0.2 mM with an initial pH as high as 11. These results are in qualitative agreement with the pH changes measured for Ca^{2+} binding to phosphatidic acids [32,40,46]. Thus, the pH-induced change in lanthanide-phosphatidic acid complexation must be a consequence of constraints imposed by the surrounding free lipid, which change with degree of protonation. Either the number of coordinating phosphates or the packing geometry changes in response to the degree of protonation of the bulk lipid.

Several attempts were made to establish the number of coordinating phosphates per bound lanthanide using ^{31}P-NMR, as done with phosphatidylcholines [21,33–36]. However, the lanthanide-phosphatidic acid complexes were found to be in slow chemical exchange, and the paramagnetic broadening of the ^{31}P resonance resulted in the bound state being undetectable under the conditions used. Analysis of the phosphate stretch region in the infrared spectrum was also attempted with these complexes but, as yet, without success.

$Ce^{3+} \rightarrow Tb^{3+}$ energy transfer and phase separation

Ce^{3+} has a strong emission band near 365 nm that overlaps with a group of Tb^{3+} 4f to 4f absorption bands and has been shown to be an efficient resonance energy donor for Tb^{3+} [30,31]. Fig. 5 shows emission spectra of a 0.007 mM Ce^{3+} and 0.007 mM Tb^{3+} mixture in 0.1 M NaCl, and the same solution with 0.25 mM DMPA at pH 7.2. Aquo-Ce^{3+} has an absorption coefficient of about 20 $M^{-1} \cdot cm^{-1}$ at 300 nm (700 $M^{-1} \cdot cm^{-1}$ at 265 nm) while that of Tb^{3+} at 300 nm is less than 0.05 $M^{-1} \cdot cm^{-1}$. As a result, the 365 nm emission of aquo-Ce^{3+} dominates the dashed-line spectrum in Fig. 5. In the Ce^{3+}/Tb^{3+}-DMPA mixed complex the Tb^{3+} 490 nm and 545 nm emission bands are 1400-times more intense than those of the aquo-species (Fig. 5) or roughly

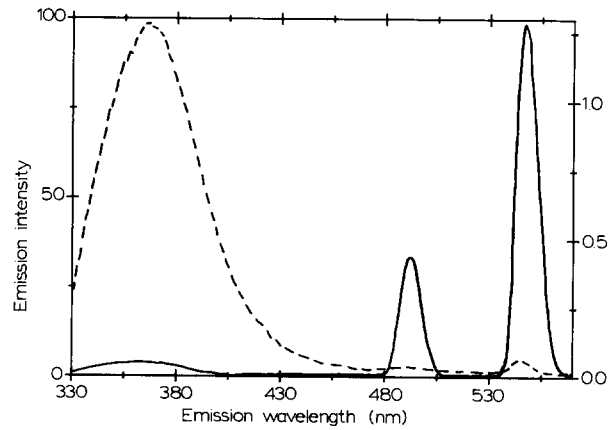

Fig. 5. Evidence for Ce^{3+} to Tb^{3+} energy transfer in phosphatidic acid complexes. In the absence of lipid the emission spectrum is dominated by the Ce^{3+} band at 365 nm (dashed line), with a band at 545 nm for Tb^{3+} barely detectable; both lanthanides are present at 0.007 mM. When bound to phosphatidic acid, excitation of Ce^{3+} results in very efficient transfer to Tb^{3+} with up to 95% quenching of the Ce^{3+} emission. Here, the Ce^{3+}/Tb^{3+}-DMPA emission spectrum is dominated by the Tb^{3+} bands at 490 and 545 nm (solid line). This spectrum is for 0.25 mM DMPA, 0.007 mM Tb^{3+}, 0.007 mM Ce^{3+}, 0.1 M NaCl, pH 7.2 and 25°C. The ordinate on the left is for the solid line spectrum and is seventy times that on the right for the dashed line spectrum.

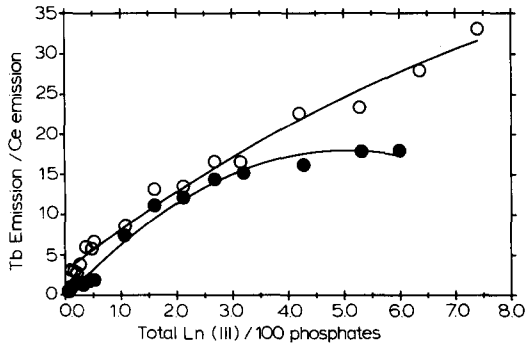

Fig. 6. Ce^{3+} and Tb^{3+} clustering as a function of lanthanide to lipid ratio, monitored by the apparent energy transfer efficiency. The ordinate is the integrated area of the Tb^{3+} 545 nm emission band divided by the area of Ce^{3+} 365 nm emission band. Direct excitation is through Ce^{3+} at 300 nm. The empty circles are for 0.25 mM DMPA and the filled circles are for 0.25 mM DOPA. Both samples were at pH 7.2 in 0.1 M NaCl and 25 °C. The samples were thoroughly sonicated after each lanthanide addition.

700-times greater than those of the Tb^{3+}-DMPA species alone [19]. Note that for the lanthanide-DMPA complex the emission scale is about seventy times greater in Fig. 5.

DMPA complexes with 1 : 1 Ce^{3+}/Tb^{3+} yield a maximum Ce^{3+} quenching of at least 95%. The remaining 5%, or less, of the Ce^{3+} emission is close to the probability of a Ce^{3+} having only other Ce^{3+} atoms as nearest neighbors in the lanthanide-rich phase. This suggests that a single nearest neighbor Tb^{3+} is sufficient for nearly complete quenching of an adjacent Ce^{3+}. Energy transfer with this efficiency is indicative of very short lanthanide-lanthanide distances in these complexes, i.e., less than 1 nm. Fig. 6 shows that this clustering of cations occurs well below 1 : 100 Ln^{3+}/lipid. The emission from Tb^{3+}-DMPA would be less than a percent of that from Ce^{3+}-DMPA if the cations were evenly dispersed on the vesicle surface.

There is ample evidence that Ca^{2+} also induces lateral phase separation in membranes containing phosphatidic acid [14,37–45]. The Ce^{3+} to Tb^{3+} energy transfer experiments allow this process to be monitored at concentrations and a timescale matched only by fluorescence studies of labeled lipids [41,44,45].

Tb^{3+} emission from the Ce^{3+}/Tb^{3+}-DOPA samples is consistently lower than that for DMPA. This could be a consequence of a lower degree of lanthanide clustering, greater separation between lanthanide centers, or a lower inherent emission efficiency for Tb^{3+}-DOPA. A more quantitative set of studies is underway in order to distinguish among these possibilities.

Kinetics studies of the growth and chelator-induced dissolution of the lanthanide-rich phase are represented in Fig. 7 for DMPA and DOPA at 25 °C and Fig. 8 for 66 °C. DOPA is fluid at both temperatures while DMPA is in the gel-state at 25 °C. At both temperatures, cluster growth is more rapid for DOPA, but dissociation of the cations from DOPA is much slower, especially at 25 °C. This is consistent with the greater tendency of DOPA to form inverted micelle structures, such as the H_{II} phase, in the presence of polyvalent cations [7–12]. Addition of EDTA to Ce^{3+}/Tb^{3+}-DMPA at 25 °C results in monotonic release of lanthanide which is effectively complete after 24 h. Ce^{3+}/Tb^{3+}-DMPA at 66 °C and Ce^{3+}/Tb^{3+}-DOPA at both temperatures do not yield complete release of lantahnide 24 h after EDTA addition. In these three cases approx. 10–20% of the initial Tb^{3+} emission persists for more than one day, an indication that the cations have become entrapped in the vesicles.

The initial stage of Ce^{3+}/Tb^{3+} clustering occurs on a subsecond timescale and very likely involves rapid release and readsorption of isolated cations, as well as lateral diffusion of the complex to a growing cluster. Subsequent growth of the clusters occurs with a half-life

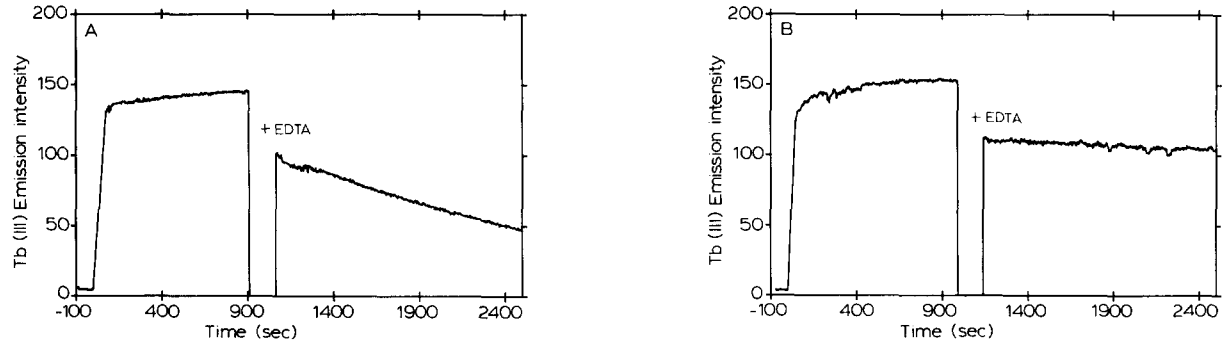

Fig. 7. Time dependence of Tb^{3+} and Ce^{3+} clustering and EDTA-induced release at 25 °C: (A) 0.25 mM DMPA, 0.004 mM Ce^{3+}, 0.004 mM Tb^{3+}, 0.1 M NaCl (pH 5.8); and (B) 0.25 mM DOPA, 0.004 mM Ce^{3+}, 0.004 mM Tb^{3+}, 0.1 M NaCl (pH 6.6). The ordinate is Tb^{3+} emission intensity (545 nm) stimulated by excitation of Ce^{3+} (300 nm). The experiments were initiated by adding 0.020 ml of a 0.2 mM Tb^{3+} and 0.2 mM Ce^{3+} solution to 1.0 ml of a thermally equilibrated suspension of sonicated lipid vesicles. The sample cell was inverted 20 times to mix and placed back in the thermally regulated cell holder with a total dead time of 30–50 s. The signal recorded at negative time is background scattering from the vesicle suspension alone. Roughly 15 min after initial mixing the cell was removed from the instrument and 0.5 ml of 31 mM EDTA (0.1 M NaCl, pH 5.7) was added, the sample mixed, and the cell returned to the instrument.

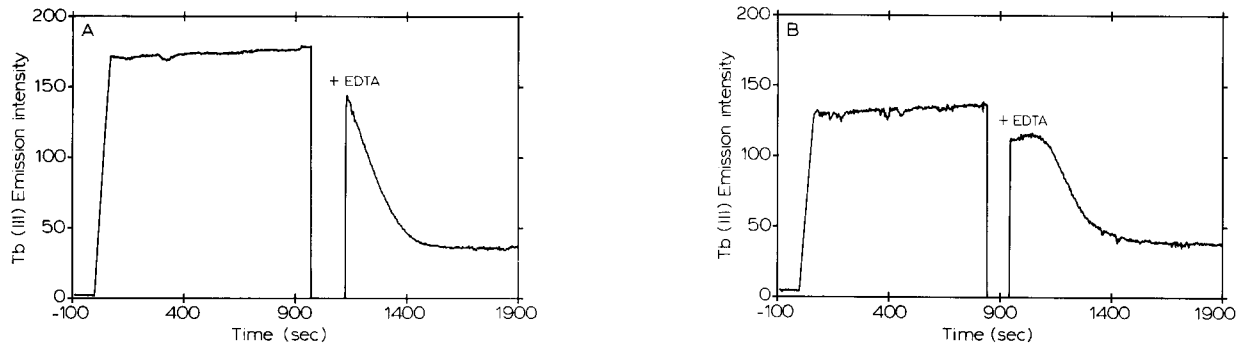

Fig. 8. Time dependence of Tb^{3+} and Ce^{3+} clustering and EDTA-induced release at 66 °C: (A) 0.25 mM DMPA, 0.04 mM Ce^{3+}, 0.004 mM Tb^{3+}, 0.1 M NaCl (pH 5.8); and (B) 0.25 mM DOPA, 0.004 mM Ce^{3+}, 0.004mM Tb^{3+}, 0.1 M NaCl (pH 6.6). The ordinate is Tb^{3+} emission intensity (545 nm) stimulated by excitation of Ce^{3+} (300 nm). Refer to the caption for Fig. 7 for details.

on the order of hours. This along with slow release of cation following addition of EDTA suggests that desorption of cations from a cluster is very slow and probably occurs only at the periphery.

Slow growth of the cation-rich phase was also observed in a study of the Tb^{3+}-DMPA infrared spectrum. The acyl-chain C-H symmetric stretch was used to monitor the gel-to-liquid crystal phase transition. In these experiments, 0.2 M DMPA in 0.1 M NaCl was placed in a thermally regulated transmission cell with ZnSe windows. The C-H stretch was found at 2852 cm^{-1} in the gel state and approx. 2854 cm^{-1} in the liquid-crystalline state, with an inflection in the temperature dependence at 42 °C. Within hours of preparing a second sample containing 0.08 M Tb^{3+}, the gel state band was still located near 2852 cm^{-1}, but the thermal transition was less cooperative and gave an inflection at 25 °C. In addition, the band shifted to only 2853 cm^{-1} at high temperature. This sample was kept at room temperature overnight and the experiment repeated. On the second day, the C-H symmetric stretch for Tb^{3+}-DMPA was found near 2851 cm^{-1} and although the band shifted to higher energy by a few tenths of a wavenumber with increasing temperature, no clear inflection was observed.

The apparent loss of the thermal transition on the second day is consistent with the calorimetric studies of Jacobson and Papahadjopoulos [37], Liao and Prestegard [46] and Graham et al. [41] for Ca^{2+} binding to phosphatidic acids and other anionic lipids. However, in a series of Raman studies, Bicknell-Brown et al. [43] reported a clear thermal phase transition for Ca^{2+}-DPPA even after 24 h equilibration. It is possible that the observable used in the Raman experiments, namely the relative intensities of two C-H stretching bands, is more sensitive to changes in acylchain packing than either calorimetry or the positions of equivalent bands in the infrared spectrum.

A more quantitative set of experiments in progress indicate that the rapid nucleation process involves formation of relatively small clusters. For DMPA at 60 °C (0.1 M NaCl, initially pH 5.3) the Ce^{3+} emission in a 1 : 1 Ce^{3+}/Tb^{3+} mixture is quenched in the first minute to approx. 15% of that in absence of Tb^{3+}, with DMPA/Ln^{3+} ratios ranging from 120 : 1 to 5 : 1. This level of Ce^{3+} quenching corresponds to formation of clusters of 3–5 cations, depending on the number of nearest neighbors assumed per cation and assuming one nearest neighbor Tb^{3+} completely quenches the Ce^{3+}. A more rigorous analysis of the Tb^{3+} quenching efficiency is underway.

Discussion

By comparing the spectral features of the luminescent lanthanides, Tb^{3+}, Eu^{3+} and Ce^{3+}, it was concluded that DOPA forms two different complexes with these cations which are very similar to two of the complexes formed with DMPA. With DOPA the two complexes coexist at comparable levels from pH 3 to pH 11 and over a wide lanthanide concentration range. In contrast, a single DMPA complex dominates above pH 8 and high lanthanide levels. These observations indicate that the difference in acylchain packing for the two lipids affects the relative populations of the complexes but apparently not the structures.

In several studies it has been reported that Ca^{2+} binding to phosphatidic acids results in a drop in pH as a consequence of deprotonation of the coordinating phosphates [32,40,46]. Not surprisingly, lanthanide binding to phosphatidic acid is also accompanied by a decrease in pH that follows the time dependence of the phase separation. The nearly equimolar coexistence of two Ln^{3+}-DOPA complexes above pH 11 indicates that the complexes do not differ in protonation of the coordinating phosphates. They must differ in stoichiometry or ligand packing. The same must be true for the equivalent pair with DMPA.

$Ce^{3+} \rightarrow Tb^{3+}$ energy transfer was observed even at 1 lanthanide per 1000 lipid molecules, indicating a strong tendency for the cations to cluster. This has also been observed in several studies of Ca^{2+}-phosphatidic acid

complexes with the cation-rich phase forming either a gel-like state [13,14,27,37–47] or inverted phases such as H_{II} [7–12,48,49]. The energy transfer experiments presented here provide two distinct advantages over most other approaches to monitoring growth of these cation-lipid phases. With Ce^{3+} as a donor, part-per-million levels of the cation-lipid clusters are readily detected, and the extent of Ce^{3+} quenching can be related to the average cluster size. Although fluorescence microscopy has been successfully used to monitor lipid phase separation [44,45], the spatial resolution limits the cluster definition to domains of several thousand lipid molecules. Even with electron microscopy it would be difficult to detect randomly distributed clusters of only five or so lipid molecules.

The maximum transfer efficiency for DMPA is greater than that for DOPA, which is a consequence of either a difference in lanthanide packing in the clusters or in the extent of cluster formation. Release of the lanthanides after addition of EDTA was consistent with the relative tendencies of DOPA and DMPA to convert to nonlamellar structures [7–12,49]. The observations with DOPA are also consistent with those of Smaal et al. [11,12] who found that Ca^{2+} is readily transported to the inside of the DOPA-containing vesicles.

The Ce^{3+} to Tb^{3+} energy transfer experiments are being explored as a means to describe cluster growth and the relation between domain size and membrane fusion events. Ce^{3+} provides the sensitivity to make this feasible and the 'fingerprint' character of the Tb^{3+} excitation spectrum provides the means to establish the lipid composition of binding sites in mixed lipid systems [19]. For example, in mixtures of phosphatidic acid and phosphatidylserine Tb^{3+} clearly binds preferentially to phosphatidic acid [50], with no sign of coordination by phosphatidylserine until the phosphatidic acid is nearly depleted.

Given that cation–lipid interactions may be important in a variety of membrane processes, continued exploitation of these unique probes should be encouraged.

Acknowledgements

This work was supported in part by a grant from the Research Corporation. We thank Dr. H.N. Halladay for the NMR and infrared data.

References

1 Copeland, B.R. and Andersen, H.C. (1981) J. Chem. Phys. 74, 2536–2547.
2 Copeland, B.R. and Andersen, H.C. (1981) J. Chem. Phys. 74, 2548–2558.
3 Copeland, B.R. and Andersen, H.C. (1982) Biochemistry 21, 2811–2820.
4 Toko, K. and Yamafuji, K. (1981) Biophys. Chem. 14, 11–23.
5 Ohki, S. (1982) Biochim. Biophys. Acta 689, 1–11.
6 Ohki, S. (1988) in Molecular Mechanisms of Membrane Fusion (Ohki, S., Doyle, D., Flanaga, T.D., Hui, S.W. and Mayhew, E., eds.), pp. 123–138, Plenum Press, New York.
7 Farren, S.B., Hope, M.J. and Cullis, P.R. (1983) Biochem. Biophys. Res. Commun. 111, 675–682.
8 Verkleij, A.J., De Maagd, R., Leunsissen-Bijvelt, J. and De Kruijff, B. (1982) Biochim. Biophys. Acta 684, 255–262.
9 Miner, V.W. and Prestegard, J.H. (1984) Biochim. Biophys. Acta 774, 227–236.
10 Verkleij, A.J. (1984) Biochim. Biophys. Acta 779, 43–63.
11 Smaal, E.B., Mandersloot, J.G., Demel, R.A., De Kruijff, B. and De Gier, J. (1987) Biochim. Biophys. Acta 897, 180–190.
12 Smaal, E.B., Nicolay, K., Mandersloot, J.G., Demel, R.A., de Gier, J. and De Kruijff, B. (1987) Biochim. Biophys. Acta 897, 453–466.
13 Portis, A., Newton, C., Pangborn, W. and Papahadjopoulos, D. (1979) Biochemistry 18, 780–790.
14 Feigenson, G.W. (1986) Biochemistry 25, 5819–5829.
15 Bentz, J., Alford, D., Cohen, J. and Düzgüneş, N. (1988) Biophys. J. 53, 593–607.
16 Saris, N.-E.L. (1983) Chem. Phys. Lipids, 34, 1–5.
17 Herrmann, T.R., Jayaweera, A.R. and Shamoo, A.E. (1986) Biochemistry 25, 5834–5838.
18 Conti, J., Halladay, H.N. and Petersheim, M. (1987) Biochim. Biophys. Acta 902, 53–64.
19 Halladay, H.N. and Petersheim, M. (1988) Biochemistry 27, 2120–2126.
20 Petersheim, M. and Sun, J. (1989) Biophys. J. 55, 631–636.
21 Petersheim, M., Halladay, H.N. and Blodnieks, J. (1989) Biophys. J. 56, 551–557.
22 Martin, R.B. and Richardson, F.S. (1979) Q. Rev. Biophys. 12, 181–209.
23 Horrocks, W. DeW. Jr. and Albin, M. (1984) Porg. Inorg. Chem. 31, 1–104.
24 Richardson, F.S. (1982) Chem. Rev. 82, 541–552.
25 Horrocks, W. DeW., Jr. and Sudnick, D.R. (1979) J. Am. Chem. Soc. 101, 334–340.
26 Petersheim, M. (1990) in Fluorescence in Biochemistry and Cell Biology (Dewey, T.G., ed.), Plenum Press, New York, in press.
27 Liao, M.-J. and Prestegard, J.H. (1980) Biochim. Biophys. Acta 601, 453–461.
28 Patil, G.S., Dorman, N.J. and Cornwall, D.G. (1979) J. Lipid Res. 20, 663–668.
29 Carnall, W.T., Fields, P.R. and Rajnak, K. (1968) J. Chem. Phys. 49, 4447–4449.
30 Reisfeld, R. (1976) in Structure and Bonding (Dunitz, J.D., Hemmerich, P., Ibers, J.A., Jørgensen, C.K., Neilands, J.B., Reinen, D. and Williams, R.J.P., eds.), Vol. 30, pp. 65–98, Springer-Verlag, Berlin.
31 Blasse, G. (1979) in Handbook on the Physics and Chemistry of Rare Earths (Gschneidner, K.A., Jr. and Eyring, L., eds.), pp. 237–274, North-Holland Publishing Company, Amsterdam.
32 Boughriet, A., Ladjadj, M. and Bicknell-Brown, E. (1988) Biochim. Biophys. Acta 939, 523–532.
33 Hauser, H., Phillips, H.C., Levine, B.A. and Williams, R.J.P. (1976) Nature 261, 390–394.
34 Grasdalen, H., Eriksson, L.E.G., Westman, J. and Ehrenberg, A. (1977) Biochim. Biophys. Acta 469, 151–162.
35 Sears, B., Hutton, W.C. and Thompson, T.E. (1976) Biochemistry 15, 1635–1639.
36 Chrzeszczyk, A., Wishnia, A. and Springer, C.S., Jr. (1981) Biochim. Biophys. Acta 648, 28–48.
37 Jacobson, K. and Papahadjopoulos, D. (1975) Biochemistry 14, 152–161.
38 Ito, T. and Ohnishi, S.-I. (1974) Biochim. Biophys. Acta 352, 29–37.
39 Galla, H.J. and Sackmann, E. (1975) J. Am. Chem. Soc. 97, 4114–4120.

40 Caffrey, M. and Feigenson, G.W. (1984) Biochemistry 23, 323–331.
41 Graham, I., Gagné, J. and Silvius, J.R. (1985) Biochemistry 24, 7123–7131.
42 Kouaouci, R., Silvius, J.R., Graham, I. and Pezolet, M. (1985) Biochemistry 24, 7132–7140.
43 Bicknell-Brown, E., Brown, K.G. and Borchman, D. (1986) Biochim. Biophys. Acta 862, 134–140.
44 Haverstick, D.M. and Glaser, M. (1987) Proc. Natl. Acad. Sci. USA 84, 4475–4479.
45 Eklund, K.K., Vuorinen, J., Kikkola, J., Virtanen, J.A. and Kinnunen, P.K.J. (1988) Biochemistry 27, 3433–3437.
46 Liao, M.J. and Prestegard, J.H. (1981) Biochim. Biophys. Acta 645, 149–156.
47 Murari, M.P., O'Brien, M.P. and Prestegard, J.H. (1988) in Molecular Mechnisms of Membrane Fusion (Ohki, S., Doyle, D., Flanagan, T.D., Hui, S.W. and Mayhew, E., eds.), pp. 25–36, Plenum Press, New York.
48 Tilcock, C.P.S., Cullis, P.R. and Gruner, S.M. (1988) Biochemistry 27, 1415–1420.
49 Cullis, P.R. and Hope, M.J. (1988) in Molecular Mechanisms of Membrane Fusion (Ohki, S., Doyle, D., Flanagan, T.D., Hui, S.W. and Mayhew, E., eds.), pp. 37–51, Plenum Press, New York.
50 Sun, J. (1990) M.S. Thesis, Seton Hall University, South Orange, NJ.